

## Fluorescent Lifetime Trajectories of a Single Fluorophore Reveal Reaction Intermediates During Transcription Initiation

Maria Sorokina,<sup>†</sup> Hye-Ran Koh,<sup>‡</sup> Smita S. Patel,<sup>§</sup> and Taekjip Ha<sup>\*,†,||</sup>

Department of Physics and Center for the Physics of Living Cells, University of Illinois at Urbana–Champaign, Urbana, Illinois 61801, Department of Chemistry, Seoul National University, Seoul 151-747, Korea, Department of Biochemistry, Robert Wood Johnson Medical School, Piscataway, New Jersey 08854, and Howard Hughes Medical Institute, Urbana, Illinois 61801

Received April 18, 2009; E-mail: tjha@illinois.edu

Single molecule (SM) techniques are relatively new additions to the field of biophysics that allow one to manipulate individual molecules and study their behavior.<sup>1</sup> To make these studies more relevant biologically, one needs to move beyond the studies of molecules in isolation and study many different molecules working in concert. This presents a technical challenge as most SM experiments measure only one observable as a function of time, whereas complex biomolecular systems require multidimensional SM analysis. Förster resonance energy transfer (FRET) is one of the most common SM approaches and can report on the real time distance changes.<sup>1</sup> However, FRET requires two fluorophores which will ultimately limit the degree of multiplexing and is subject to changes in the local environment.<sup>2</sup> It will be useful if a single fluorophore can provide equivalent information. In this communication, we show that fluorescence lifetime analysis of a single Cy3 fluorophore attached to the promoter region of the DNA can reveal transient reaction intermediates during transcription initiation by T7 RNA polymerase. This work represents the first demonstration of real-time biochemical reactions observed via single molecule fluorescence lifetime trajectories of immobilized molecules.

We used a picosecond mode-locked laser and time correlated single photon counting (TCSPC)<sup>3</sup> to determine the time delay between the excitation laser pulse and the single photon emitted by a DNA-conjugated Cy3 fluorophore during RNA transcription by the T7 RNA polymerase (RNAP). T7 RNAP is a single subunit enzyme that catalyzes all steps of transcription including initiation, elongation, and termination.<sup>4</sup> Here, we focused on the initiation process, which consists of several key steps. It starts from binding of the RNAP to a promoter site on the DNA molecule,<sup>5</sup> followed by the internal melting/unwinding to create a transcription bubble.<sup>6</sup> The RNAP then synthesizes short RNA molecules (<12 nt) while staying in contact with the promoter site, thereby scrunching in the downstream DNA, and occasionally releases the short RNA to restart RNA synthesis in a process called abortive initiation.<sup>7</sup> After a stochastic number of abortive cycling, the RNAP undergoes a major conformational change, accompanied by the promoter release, to change into an elongation complex where it synthesizes the RNA molecule in a highly processive manner.<sup>8,9</sup> These reaction intermediates create different environments for Cy3 attached to the -4 position of the nontemplate strand of the promoter region of the DNA (Figure 1A), changing the fluorescence lifetime in ways that can be differentiated using TCSPC.

We used a home-built confocal scanning microscope to locate single Cy3-labeled DNA molecules tethered to a polymer-passivated

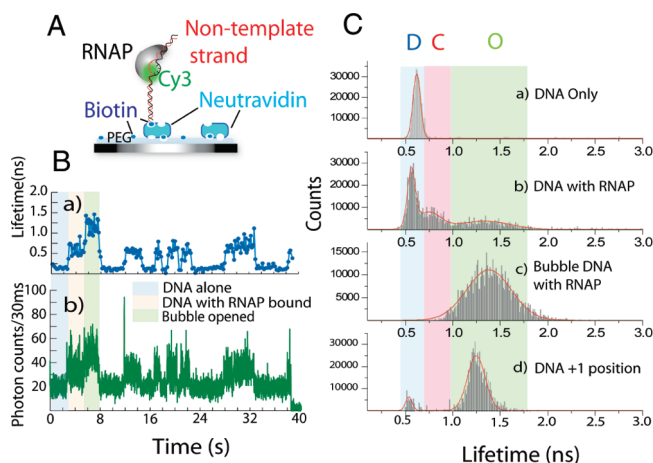


**Figure 1.** Transcription bubble opening: (A) Schematic of the experiment. (B) Example of the corresponding SM lifetime trace, demonstrating successive RNAP binding and transcription bubble opening events. (C) (a) SM lifetime distribution histogram of Cy3 conjugated to -4 position of the nontemplate strand shows a peak at 0.6 ns, consistent with bulk solution data (SI). (b) Three peaks are distinguished when RNAP is added to the solution. (c) The lifetime distribution of Cy3 conjugated to the bubble DNA (SI) with RNAP in the solution suggests that the third peak in (b) corresponds to the opened DNA–RNAP complex. (d) After adding 3'-dGTP, RNAP is stalled at position +1/+2.

glass coverslip (Figure 1A)<sup>10</sup> and to record both the intensity and lifetime trajectories of each molecule [Supporting Information (SI), Figure S1]. The delay time intervals were collected into histograms with 500 photons in each and then fitted with a single exponential decay function using the maximum likelihood estimator algorithm.<sup>11</sup> Lifetime histograms were built from ~50 molecules under each condition (Figure 1C). With DNA-only and no RNAP present, a single narrow peak at 0.6 ns was observed (Figure 1Ca),<sup>12</sup> in agreement with our bulk solution data [SI, Figure S2, Table S1]. After adding 10 nM RNAP to the solution, two additional peaks emerged (Figure 1Cb). One was centered at 0.8 ns and is attributed to the closed DNA–RNAP complex in which the transcription bubble has not formed. We propose that the second peak, centered at 1.3 ns, is due to the open complexes with the bubble formed. T7 RNAP is capable of opening the transcription bubble even in the absence of NTPs.<sup>6</sup> We confirmed that the 1.3 ns value corresponds to the open complex using two methods. First, we performed the same experiment using premelted DNA molecules [SI, Table S2] having six unpaired base pairs and found that the lifetime is broadly distributed and is centered at 1.4 ns (Figure 1Cc), also in agreement with our bulk solution data [SI, Figure S2]. Second, to make sure that the bubble is formed, we added 3'-dGTP to our standard DNA with a fully base paired duplex, thereby stalling the RNAP at the

<sup>†</sup> University of Illinois at Urbana–Champaign.

<sup>‡</sup> Seoul National University.

<sup>§</sup> Robert Wood Johnson Medical School.

<sup>||</sup> Howard Hughes Medical Institute.

+1/+2 position and found a narrowly distributed lifetime centered at 1.25 ns (Figure 1Cd). These control measurements support the conclusion that RNAP can open the bubble even in the absence of NTPs (Figure 1Cb). The broad distribution of the lifetime, however, suggests that the open complex in the absence of NTPs is not stable and the RNAP–DNA complex is likely to fluctuate between closed and opened forms. Such fluctuations are suppressed when RNAP moves forward to the +1/+2 position (Figure 1Cd).

An example SM time trace of lifetime shows the real time dynamics of RNAP binding and opening of the transcription bubble without NTP (Figure 1Ba). It starts with the DNA-only value of 0.6 ns, and at  $t = 3$  s, an RNAP binds raising the lifetime to 0.8 ns. A stable transcription bubble is formed 3 s later with the lifetime at  $\sim 1.3$  ns. This open complex collapses after  $\sim 2$  s, quickly followed by RNAP dissociation. RNAP binding does not always lead to a stable bubble opening as the subsequent fluctuations between 0.6 and 0.8 ns indicate. The simultaneously obtained fluorescence intensity time trace shows the same behavior (Figure 1Bb) and can even detect short-lived open states that the lifetime traces could not reveal.<sup>13</sup>

The DNA scrunching model states that RNAP can synthesize up to 12 nt long RNA while staying bound to the promoter site.<sup>14,15</sup> The growing RNA is accumulated inside the RNAP pocket, and the elastic energy thus built up is proposed to result in promoter release and transition to the elongation phase. We asked if DNA scrunching during initial transcription may be detected through the change in the Cy3's local environment, and therefore its fluorescence lifetime. We stalled RNAP at defined positions using a limiting mixture of NTPs and NTP analogues at saturating concentrations (SI, Table S2) and built the lifetime histograms (Figure 2A). The histogram obtained with 10 nM RNAP without any NTPs shows three peaks, as discussed earlier, corresponding to DNA-only and the closed and open complexes. Starting from the +1/+2 position, the closed complex peak vanishes, indicating that all of the DNA–RNAP complexes are in the open state. For the +8 and +9 positions the distribution shows two populations with the major peak showing up at  $\sim 1.6$  ns, likely due to the conformational change toward the elongation complex that starts to happen at these positions.<sup>13</sup> The near absence of population at 0.6 ns up to the +9 position and the longer lifetime which is generally an indication of higher local viscosity<sup>16</sup> suggest that the 1.6 ns lifetime state likely presents an intermediate structure between the initiation and the elongation complex where the promoter site remains in high proximity to the protein.<sup>17</sup>

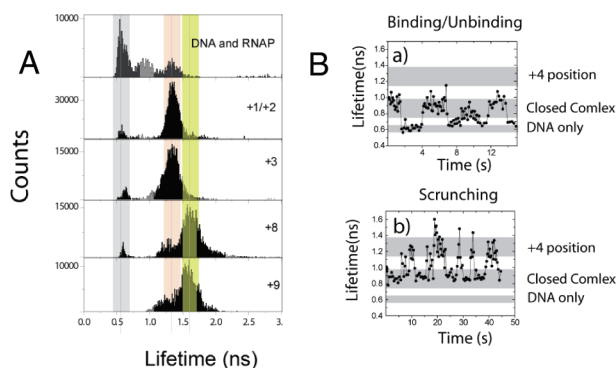


**Figure 2.** (A) Lifetime distributions for different RNAP stall positions. Starting from the +1/+2 position, the lifetime increases until the +9 position. (B) Two lifetime traces displaying different processes: (a) RNAP binding and unbinding. (b) The LT trace for the molecule that observes a repeated scrunching/unscrunching process.

Using the lifetime trajectories, we can distinguish between scrunching/unscrunching and binding/dissociation processes (Figure 2Ba,b). Unscrunching occurs when a short RNA product is released so that the RNAP active site returns to the +0 position (and associated decrease in lifetime). To observe the scrunching/unscrunching dynamics, we slowed down the RNA synthesis rate by decreasing the NTP concentrations to 10  $\mu$ M, and applied a limiting NTP mixture so that RNA product can not be longer than 4 nt (Figure 2Bb). Under these conditions, two types of behavior were observed. In the first, binding and dissociation of RNAP molecules were detected without any evidence of active transcription (Figure 2Ba). In the second, repetitive scrunching/unscrunching events are seen as lifetime fluctuations during which the lifetime never drops to the DNA-only value, indicating that the RNAP stays bound to the DNA between adjacent cycles of abortive RNA synthesis (Figure 2Bb).

In summary, we demonstrated that it is possible to study biological processes as complex as transcription initiation using only one fluorophore at the SM level as opposed to using two fluorophores.<sup>15,18</sup> This was achieved by applying the SM TCSPC to the surface immobilized molecules. Although SM TCSPC was used previously for molecules diffusing in solution<sup>19</sup> and to observe photophysical dynamics of immobilized molecules,<sup>11</sup> it has never been used to observe the real time biochemical reactions from surface-tethered molecules until this study. In particular, we were able to observe transcription bubble opening and abortive RNA synthesis during transcription initiation. Because the fluorescence lifetime is directly proportional to the quantum yield of Cy3,<sup>16</sup> in principle a Cy3 intensity measurement alone could be enough as was the case for monitoring the repetitive motion of a translocase.<sup>20</sup> In practice, however, it is difficult to calibrate the intensity signal due to various sources of intensity variation, whereas the lifetime measurement does not suffer from these problems.

**Acknowledgment.** We thank the NIH (GM65367, GM51966) and NSF (0822613) for funding and Rahul Roy for advice.

**Supporting Information Available:** Detailed description of the confocal and TCSPC setup, experimental protocols, results of the bulk experiments. This material is available free of charge via the Internet at <http://pubs.acs.org>.

## References

- Joo, C.; Balci, H.; Ishitsuka, Y.; Buranachai, C.; Ha, T. *Ann. Rev. Biochem.* **2008**, *77*, 51.
- Hinze, G.; Metivier, R.; Nolde, F.; Mullen, K.; Basche, T. *J. Chem. Phys.* **2008**, *128*, 124516.
- Felekyan, S.; Kuhnemuth, R.; Kudryavtsev, V.; Sandhagen, C.; Becker, W.; Seidel, C. A. M. *Rev. Sci. Instrum.* **2005**, *76*, 083104.
- Murakami, K. S.; Darst, S. A. *Curr. Opin. Struct. Biol.* **2003**, *13*, 31.
- Bandwar, R. P.; Jia, Y.; Stano, N. M.; Patel, S. S. *Biochemistry* **2002**, *41*, 3586.
- Tang, G. Q.; Patel, S. S. *Biochemistry* **2006**, *45*, 4936.
- Tang, G. Q.; Roy, R.; Ha, T.; Patel, S. S. *Mol. Cell* **2008**, *30*, 567.
- Durmiak, K. J.; Bailey, S.; Steitz, T. A. *Science* **2008**, *322*, 553.
- Yin, Y. W.; Steitz, T. A. *Science* **2002**, *298*, 1387.
- Ha, T. *Methods* **2001**, *25*, 78.
- Edel, J. B.; Eid, J. S.; Meller, A. J. *Phys. Chem. B* **2007**, *111*, 2986.
- Sanborn, M. E.; Connolly, B. K.; Gurunathan, K.; Levitus, M. *J. Phys. Chem. B* **2007**, *111*, 11064.
- Hye Ran Koh, manuscript in preparation.
- Revyakin, A.; Liu, C.; Ebright, R. H.; Strick, T. R. *Science* **2006**, *314*, 1139.
- Kapanidis, A. N.; Margeat, E.; Ho, S. O.; Korkhonia, E.; Weiss, S.; Ebright, R. H. *Science* **2006**, *314*, 1144.
- Aramendia, P. F.; Negri, R. M.; Sanroman, E. *J. Phys. Chem.* **1994**, *98*, 3165.
- Mukherjee, S.; Brieba, L. G.; Sousa, R. *Cell* **2002**, *110*, 81.
- Kapanidis, A. N.; Margeat, E.; Laurence, T. A.; Doose, S.; Ho, S. O.; Mukhopadhyay, J.; Korkhonia, E.; Mekler, V.; Ebright, R. H.; Weiss, S. *Mol. Cell* **2005**, *20*, 347.
- Edman, L.; Mets, U.; Rigler, R. *Proc. Natl. Acad. Sci. U.S.A.* **1996**, *93*, 6710.
- Myong, S.; Cui, S.; Cornish, P. V.; Kirchofer, A.; Gack, M. U.; Jung, J. U.; Hopfner, K. P.; Ha, T. *Science* **2009**, *323*, 1070.

JA902861F